Materials Science & Engineering A 735 (2018) 354–360

Contents lists available at ScienceDirect

Materials Science & Engineering A

journal homepage: www.elsevier.com/locate/msea

Segregation induced hardening in annealed nanocrystalline Ni-Fe alloy

N. Zhang[a], S.B. Jin[b], G. Sha[b], J.K. Yu[a], X.C. Cai[a], C.C. Du[a], T.D. Shen[a,*]

[a] Clean Nano Energy Center, State Key Laboratory of Metastable Materials Science and Technology, Yanshan University, Qinhuangdao 066004, PR China
[b] Herbert Gleiter Institute of Nanoscience, Nanjing University of Science and Technology, Nanjing 210094, PR China

ARTICLE INFO

Keywords:
Nanocrystalline metal
Annealing hardening
Grain boundary segregation
Atom probe tomography

ABSTRACT

Annealing often causes softening in conventional large-grained materials. However, annealing has been found to cause hardening in many nanocrystalline metals and alloys. This abnormal hardening by annealing has been explained by such factors as solute segregation at grain boundaries, grain boundary relaxation, grain boundary pinning by second phase particles, etc. In the present work, a homogenous single-phase nanocrystalline Ni(Fe) alloy prepared by electrodeposition was investigated. This alloy is with approx. 1 at% Fe and composed of a solid solution of Fe in Ni without any precipitated phase. The goal is to shed light on which mechanism dominates annealing hardening. Microhardness of the alloy was found to increase slightly just before the grains started to grow during annealing. In addition, long time annealing at the hardening temperature resulted in the decrease of hardness due to grain growth. Both lattice parameter and atom probe tomography studies suggest that the annealing hardening is caused by the segregation of solute and impurity atoms on grain boundaries in the nanocrystalline Ni(Fe) alloy.

1. Introduction

For conventional polycrystalline materials, hardness, H, is related to the average grain size, d, based on the well-known Hall-Petch relationship [1,2]:

$$H = H_o + kd^{-1/2} \quad (1)$$

where H_0 and k are material constants. In addition, the well-known work hardening theory predicts that the shear strength, τ, of a plastically deformed metal increases with dislocation density, ρ, according to [3]:

$$\tau = \tau_0 + \alpha G b \rho^{1/2} \quad (2)$$

where τ_0 and α ($\approx$ 0.2–0.3) are material constants, G is the shear modulus and b is the magnitude of Burger's vector of dislocations. Annealing often increases the grain size and/or decreases the dislocation density. Thus, the hardness or strength of polycrystalline materials decreases with annealing.

However, an unusual "hardening by annealing" phenomenon has been reported in the past decades for a number of nanocrystalline (NC) metals such as nickel [4–14], iron [4,10,15], magnesium [16], copper [17], steel [18,19], titanium [20,21], aluminum [22] and high-entropy alloy [23]. These NC metals and alloys are prepared by such different techniques as mechanical alloying (MA) [4,10,14,15], electrodeposition (ED) [5–9,11,13], severe plastic deformation (SPD) [16,18,19,21,23], rolling [17,20,22], and gas deposition (GD). Several mechanisms have been proposed for the origin of hardening by annealing. i) Many researchers attributed the hardening by annealing to the segregation of solutes or impurities to grain boundaries (GBs) [4,6–10,15,16]. Molecular dynamics simulation [24–28] also suggested that dopant segregation was primarily responsible for stabilizing grain boundary. ii) Other researches proposed [5,11,18,21,22] that grain boundary relaxation, i.e., a change in the grain boundary structure retarding the motion of dislocations, caused the annealing hardening. iii) Darling and Kecskes proposed [14] that the GB stabilization through pinning by second phase particles resulted in the hardening by annealing in their Ni-Y alloys. In particular, Renk et al. [18] disagreed with the GB segregation mechanism without investigating the effect of grain size on the hardness of their NC steel.

In this work, we prepared a single-phased NC Ni(Fe) alloy with approx. 1 at% solute Fe atoms by electrodeposition. The content of Fe atoms is so low that there is no precipitation of the second phase. This excludes the effect of precipitated phase on the hardness of our NC alloy after annealing. The as-prepared Ni(Fe) alloy has an average grain size of ~ 15 nm. Isochronal and isothermal heat treatments were performed to investigate the microhardness-microstructures relation in our NC Ni (Fe) alloy. The microstructures were characterized by x-ray diffraction, transmission electron microscopy, and atom probe tomography

* Corresponding author.
E-mail address: tdshen@ysu.edu.cn (T.D. Shen).

https://doi.org/10.1016/j.msea.2018.08.061

Available online 20 August 2018

techniques. Our goal is to understand the origin of hardening in annealed NC Ni(Fe) alloy.

2. Experimental method

The NC Ni(Fe) alloy was deposited from a bath containing 300 g l^{-1} nickel aminosulfonate, 5 g l^{-1} iron dichloride, 40 g l^{-1} boric acid, 25 g l^{-1} sodium citrate, 5 g l^{-1} saccharin, 2 g l^{-1} ascorbic acid and 0.2 g l^{-1} sodium dodecyl sulfate. The voltage was pulsed with an on time of 2 ms and an off time of 15 ms and adjusted to give a current density of 0.02–0.2 A cm^{-2} during the on time. The bath temperature was 55–65 °C and the pH of plating solution was 2.8–3.6. A copper substrate was used as the cathode whereas high purity Ni (99.98%) was used as the anode. The substrate was cleaned with detergent and alkali liquid and then activated with 20% sulfuric acid before depositing. The pH of plating solution was adjusted with 200 g l^{-1} sodium hydroxide or 10% sulfamic acid to keep it in the target range. Thickness of the deposited layer was typically 1.5 mm. The electrodeposited specimens were cut using an electro-discharging machine. Isochronal (1 h) and isothermal heat treatment were carried out in an argon-filled glove box containing less than 1 ppm oxygen. After annealing, the specimens were rapidly cooled inside the glove box.

Table 1 lists composition of the electrodeposited NC Ni(Fe) alloy. Sulfur and carbon impurities in the sample were determined by a CS-8800 carbon sulfur analyzer. Other elements were analyzed by iCAP 6300 Radial ICP. The detected content of Fe is 1.34 at%. For simplicity, we named the NC alloy as $Ni_{99}Fe_1$. The carbon and sulfur impurities originated from the bath additives such as saccharin ($C_7H_4NO_3S$) used in the electro-deposition whereas the metallic impurities such as cobalt resulted from the anode material.

The microhardness (H_v) was measured on a FM-ARS-9000 Vickers hardness tester using loads of 300–500 g and dwelling time of 10 s. A constant load was used for each sample. Each reported H_v is the average of eleven separate measurements.

Average grain size, lattice parameter and dislocation density were extracted from the x-ray diffraction (XRD) patterns collected on a D/MAX-2500/PC diffractometer using Cu Kα radiation (λ = 0.15406 nm) and a graphite monochromator with scanning angle (2θ) from 40° to 102°. Step size and counting time per step were 0.02° and 2 s, respectively. Calibration of the XRD results was done with a standard Si sample. After removing instrumental broadening, crystallite sizes (D) and micro-strain (ε) were calculated from the well-known William-Hall plot [29]:

$$\beta \cos\theta = k\,\lambda/D + 2\,\varepsilon \sin\theta \quad (3)$$

where β is the peak width measured in terms of full width at half maximum (FWHM), θ is the Bragg angle, k is a constant taken as 0.9, and λ is the wavelength of the incident radiation taken as 0.15406 nm. The lattice parameters were calculated from the peak position using the Nelson-Riley method [30].

The microstructures were also studied by JEOL 2010 transmission electron microscopy (TEM) operating at 200 keV. TEM specimens were prepared by mechanically thinning and polishing, followed by ion-milling using a gatan precision ion polishing system.

Atom probe tomography (APT) was carried out to analyze the solute distribution at GBs and in grain interiors. Two sharp needle-like samples were prepared by using a standard two-stage electro-polishing procedure from blanks (0.5 mm x 0.5 mm x 10 mm in dimension) cut from as-deposited sample and annealed sample. APT experiments were performed using a Local Electrode Atom Probe (LEAP4000X Si) with a UV laser pulse repetition rate of 200 kHz, pulse laser energy of 60 pJ, a target evaporation rate of 0.5%, a specimen temperature of 20 K, a pulse rate of 250 kHz and under a high vacuum of 10^{-12} Torr. The LEAP instrument used in the current work has a detection efficiency of 55%. Reconstruction and visualization of the APT data were performed using the Imago Visualization and Analysis Software (IVAS) package (version 3.6.8).

Table 1
Composition of as-deposited NC Ni(Fe) alloy.

Element	wt%	at%
Fe	1.28	1.34
Co	0.248	0.25
Si	0.185	0.38
Ta	0.0590	0.02
Cu	0.0240	0.02
Zn	0.0170	0.02
Mn	0.0071	0.01
C	0.0777	0.38
S	0.0954	0.17

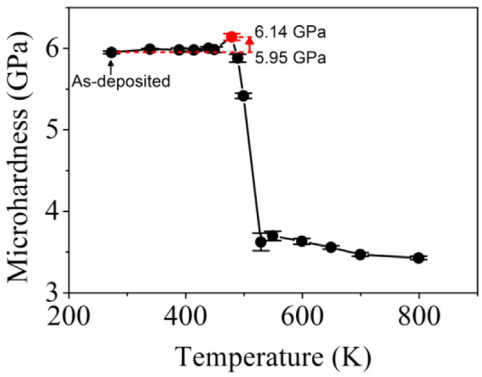

Fig. 1. Microhardness, H_v, as a function of annealing temperature for NC $Ni_{99}Fe_1$ alloys annealed for 1 h. Two horizontal dotted lines represent the microhardness of as-deposited (5.95 GPa) and annealed at 479 K (6.14 GPa) respectively.

3. Results

H_v of the NC $Ni_{99}Fe_1$ alloy before and after annealing for 1 h at selected temperature is shown in Fig. 1. The error bars are very small, indicating that the microstructure of NC $Ni_{99}Fe_1$ alloy is very uniform. H_v (~ 5.95 GPa) remains almost constant when the annealing temperature is below 449 K. H_v increases slightly to 6.14 GPa at 479 K. Then, H_v largely decreases from 6.14 GPa to 3.62 GPa between 479 K and 529 K. Finally, H_v slightly decreases between 529 K and 799 K.

Fig. 2 shows the average grain size and micro-strain of NC $Ni_{99}Fe_1$ alloy as a function of annealing temperature. The grain size and micro-strain are calculated from the William-Hall plot. The initial grain size and micro-strain are 14.6 ± 0.1 nm and 0.41 ± 0.003%, respectively. For annealing temperatures below 479 K, both the grain size and micro-

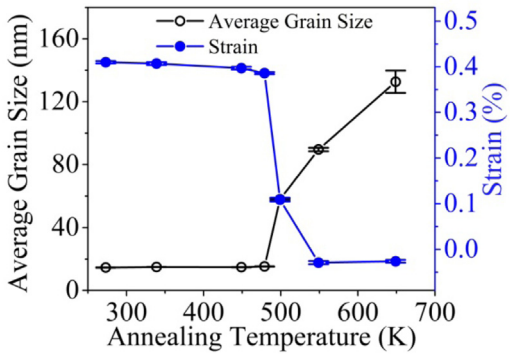

Fig. 2. Average grain size and micro-strain as a function of annealing temperature.